Protactinium-231 Dating of Carbonates by Thermal Ionization Mass Spectrometry: Implications for Quaternary Climate Change

R. Lawrence Edwards, H. Cheng, M. T. Murrell, S. J. Goldstein

Measurement of protactinium-231 (^{231}Pa) in carbonates by thermal ionization mass spectroscopy yields ^{231}Pa ages that are more than 10 times more precise than those determined by decay counting. Carbonates between 10 and 250,000 years old can now be dated with ^{231}Pa methods. Barbados corals that have identical ^{231}Pa and thorium-230 (^{230}Th) ages indicate that the timing of sea level change over parts of the last glacial cycle is consistent with the predictions of the Astronomical Theory. Two Devils Hole calcite subsamples record identical ^{231}Pa and ^{230}Th ages, suggesting that the chronology of this climate record is accurate.

The development, 10 years ago, of thermal ionization mass spectrometric (TIMS) techniques for measuring the abundance of ^{230}Th (half-life = 75,400 years) and ^{234}U (half-life = 244,500 years) resulted in large improvements in analytical sensitivity and precision (*1*). This method led to improved precision in ^{230}Th age determination, which is based on the shift in the ^{230}Th/^{234}U ratio as a result of radioactive decay (*1*). This technique has been used to obtain a high-resolution record of sea level change over parts of the past 200,000 years (*1–6*), to calibrate parts of the ^{14}C time scale (*4–5*), and to obtain a continental climate record at Devils Hole, Nevada, extending back over 500,000 years (*7*). One difficulty in interpreting ^{230}Th ages is that open-system behavior can cause shifts in the ^{230}Th/^{234}U ratio, resulting in inaccurate ages. The accuracy of ^{230}Th-based chronologies is a key issue in our understanding the Quaternary glacial cycles. The timing of sea level changes (*1–4*, 6) supports the notion that Quaternary climate change was driven by variations in Earth's orbital geometry, whereas the timing of the Devils Hole record seems to contradict this notion (*7*).

To test the accuracy of the ^{230}Th dates, we used the ^{231}Pa [half-life = 32,700 years (*8*)] chronometer. The ^{231}Pa ages are based on the change in the ^{231}Pa/^{235}U ratio resulting from radioactive decay of ^{235}U to ^{231}Pa. The ^{231}Pa age equation is $t = -\ln(1 - [^{231}\text{Pa}/^{235}\text{U}])/\lambda$, where t is the time elapsed since ^{231}Pa-^{235}U closure, λ is the decay constant for ^{231}Pa, and the brackets indicate an activity ratio. The ^{231}Pa age is accurate if (i) the initial ^{231}Pa/^{235}U ratio is zero and (ii) the ^{231}Pa/^{235}U ratio has only changed by radioactive ingrowth and decay. In addition to providing a check for ^{230}Th ages, the ^{231}Pa chronometer has other advantages. The parents of ^{230}Th and ^{231}Pa are isotopes of the same element, uranium (U), and in low-temperature geologic settings, the daughters, Pa and Th, can have similar chemical properties. Thus, the systematics of Pa-Th dating are analogous to those of U-Pb (lead) dating (*9*). Potentially, combined Pa-Th dating of Quaternary carbonates could become what U-Pb dating is to zircons (*9*); that is, similar concordia plots apply and, for discordant materials, it may be possible to obtain both primary and diagenetic ages as well as constraints on the nature of the diagenetic process (*10*).

Originally developed about 30 years ago (*11*), the main impediment for ^{231}Pa dating has been the inability to measure ^{231}Pa with sufficient precision by radioactive decay counting techniques, in which only one out of 10^6 to 10^7 ^{231}Pa atoms in a sample can be detected (for a counting time of 1 week). Here we have applied TIMS techniques, for which ionization efficiencies approaching 10^{-2} can be achieved (*12*), so that more than 1 out of 1000 ^{231}Pa atoms in a sample can be detected in a 2-hour counting time.

We dated (*13*) 32 corals from localities around the world and two subsamples of Devils Hole inorganic calcite that had previously been analyzed for ^{238}U, ^{234}U, ^{230}Th, and ^{232}Th. We also remeasured U and Th nuclides on many samples in order to have data for all nuclides on the same solutions (*13*). We chose samples with a range of ages so that we could determine ^{231}Pa age precision as a function of age (Fig. 1). Six of the corals were younger than 1000 years old and were analyzed to test the assumption that the initial ^{231}Pa/^{235}U ratio in corals is zero (Fig. 2). The other samples were analyzed because they are critical for understanding some facet of Quaternary climate change.

For our analyses (Fig. 1), the 2σ error in ^{231}Pa concentration varied from ±5% for 2.5 g of 130-year-old coral containing 13 million atoms of ^{231}Pa to ±0.8% for 3.0 g of 970-year-old coral containing 41 million atoms of ^{231}Pa to ±0.5% for 2 to 3 g of coral older than 10,000 years containing 1 to 7 billion atoms of ^{231}Pa. When these errors are propagated through the ^{231}Pa age equation, the 2σ errors in ^{231}Pa age (Fig. 1) are ±7 to ±12 years for samples younger than 2000 years, ±60 to ±120 years for samples between 8000 and 13,000 years old, ±1000 to 1400 years for samples about 80,000 years old, and ±10,000 to 17,000 years for samples 200,000 years old. For samples with ages less than 130,000 years, errors in ^{231}Pa age are typically within a factor of 3 of errors in ^{230}Th age determined by TIMS techniques (Fig. 1), even though the parent of ^{231}Pa is more than two orders of magnitude less abundant than the parent of ^{230}Th (^{238}U/^{235}U = 137.88).

All samples younger than 1000 years had ^{232}Th concentrations lower than 200 parts per trillion and ^{234}U/^{238}U ratios identical to that of modern marine U. Corals with these characteristics have been shown to record accurate ^{230}Th ages (*14*). The ^{231}Pa ages of all six samples are within error of their ^{230}Th ages, indicating that the initial ^{231}Pa/^{235}U ratio was not measurably greater than zero (Fig. 2). The average difference (^{231}Pa age minus ^{230}Th age) is 0.5 ± 4 years. The maximum observed age difference of 4.5

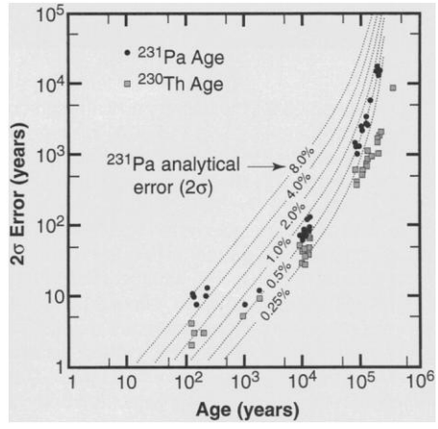

Fig. 1. $2\sigma_{mean}$ error in age versus age for coral analyses using TIMS techniques. Both axes are logarithmic. Circles represent ^{231}Pa ages; squares represent ^{230}Th ages. The percentage error in ^{231}Pa analysis is contoured and pertains only to the Pa data points. The TIMS ^{231}Pa analyses and ages are more than 10 times more precise than traditional decay counting determinations. Errors in TIMS ^{231}Pa age approach those of ^{230}Th age for materials about 10,000 years old. Errors in ^{231}Pa age are within a factor of 3 of errors in ^{230}Th age for materials younger than 130,000 years.

R. L. Edwards and H. Cheng, Minnesota Isotope Laboratory, Department of Geology and Geophysics, University of Minnesota, Minneapolis, MN 55455, USA.
M. T. Murrell and S. J. Goldstein, Chemical Science and Technology Division, Los Alamos National Laboratory, Los Alamos, NM 87545, USA.

years is equivalent to an initial $^{231}Pa/^{235}U$ activity ratio of $<9 \times 10^{-5}$ (atomic ratio $<5 \times 10^{-10}$), or an initial ^{231}Pa concentration of <200,000 atoms per gram. The assumption that the initial $^{231}Pa/^{235}U$ ratio is zero appears to be valid for reef-building corals with low concentrations of ^{232}Th.

For a ^{231}Pa age to be accurate, the $^{231}Pa/^{235}U$ ratio should only have changed by radioactive production and decay; that is, chemical reactions should not have shifted the $^{231}Pa/^{235}U$ ratio. We tested this assumption by comparing ^{231}Pa ages with ^{230}Th ages, which are also subject to a similar assumption. Thus, a comparison of a ^{231}Pa age with a ^{230}Th age is a consistency test: If a sample has identical ^{231}Pa and ^{230}Th ages, we have more confidence that the age is accurate than we would with just the ^{230}Th age. If the ages do not agree, one or both must be inaccurate. In this case, it may be possible to constrain the true age as well as the nature of the process that disturbed the system.

As compared to U-Pb systematics, models for continuous or instantaneous loss of U are the same (*10*) (Fig. 3) if ^{234}U does not fractionate from ^{235}U. However, models for U gain must be modified to account for the possibility that added U could have a different $^{234}U/^{235}U$ ratio than primary U. In either case, the isotopic composition of the gained or lost U may be constrained by the measured isotopic composition of U, if there is independent knowledge of the initial U isotopic composition (for example, if the U is marine). Models for daughter gain are similar to those for U-Pb, with different ratios of gained Pa and Th equivalent to different isotopic compositions of gained Pb. Models for daughter loss are also similar but must account for fractionation of Pa from Th. The systematics of Pa-Th are discussed in more detail elsewhere (*10*).

The other 26 corals, with ages from 1000 to 500,000 years, were screened by x-ray diffraction, and none contained detectable calcite (*5*, *6*). All but eight have initial $\delta^{234}U$ values within 8 per mil of that of marine U (*5*, *6*). Corals that are 1000 to 15,000 years old (Fig. 3) are from the Huon Peninsula, Papua New Guinea (*5*). Of these, 10 out of 13 have concordant ages, and three have slightly discordant ages. Two samples from the land surface plot just to the right of concordia (Fig. 3A, only one depicted). One sample [38.0 m (*5*)], collected by drilling into the Holocene terrace, lies just to the left of concordia (Fig. 3A). The isotopic characteristics of the surface samples with discordant ages are consistent with U gain, whereas those of the drill-core sample with a discordant age are consistent with U loss. As the initial U isotopic compositions of all three are indistinguishable from that of marine U, the Pa-Th discordance is the only evidence that these samples have behaved as open systems. The 13 samples are a subset of those used to establish that atmospheric $^{14}C/^{12}C$ ratios dropped during the Younger Dryas period, determined on the basis of ^{230}Th dating alone (*5*). As most of these samples record concordant Pa and Th ages, the Pa data support the chronology of that work.

We also used ^{231}Pa measurements to test ^{230}Th ages of corals (>80,000 years old) collected from the surface on Barbados (*6*). Five of 13 samples have concordant ages. Of those with discordant ages, all plot above concordia (Fig. 3B), and all but one have initial $\delta^{234}U$ values higher than the marine value. The nature of this discordance can be constrained by examining three samples collected from the Rendezvous Hill Terrace (last interglacial). Two (FU-1 and AFM-20, collected near the terrace surface) have concordant ages, whereas the third (FU-3, collected in a road-cut a few meters below the terrace surface) has a discordant age. The ^{230}Th age of FU-3 is much older than the others, and its $^{231}Pa/^{235}U$ ratio is greater than 1. Because these samples should be broadly correlative, these relations require that FU-3 lost U or gained Pa and Th. However, the process must be more complex because the initial $\delta^{234}U$ value of FU-3 is 90 per mil higher than the $\delta^{234}U$ of seawater. Thus, a component with a $\delta^{234}U$

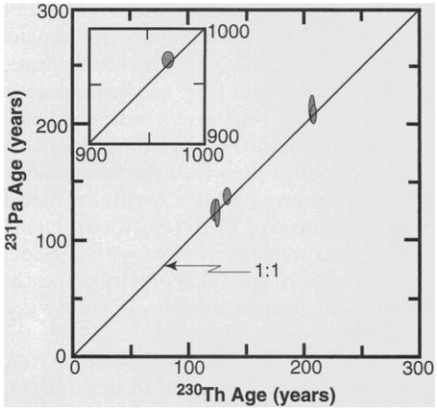

Fig. 2. ^{231}Pa versus ^{230}Th age for six coral subsamples less than 1000 years old. If significant initial ^{231}Pa were incorporated during coral growth, the data would plot systematically above the 1:1 line. The corals all have ages that plot within error of the 1:1 line, consistent with the assumption that the initial $^{231}Pa/^{235}U$ ratio in these corals is effectively zero and indicating that the ages are accurate.

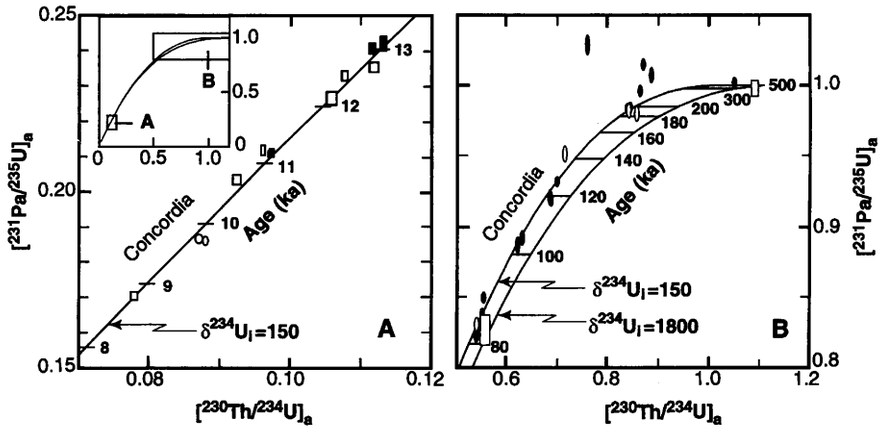

Fig. 3. Plots of $^{231}Pa/^{235}U$ activity versus $^{230}Th/^{234}U$ activity (Pa-Th concordia plots) for (**A**) Huon Peninsula, Papua New Guinea corals (*5*), and (**B**) Barbados corals (*6*) and two Devils Hole inorganic calcite subsamples (*7*). Circles and ellipses indicate corals collected on the surface; squares in (A) indicate corals collected by drilling; squares in (B) represent Devils Hole subsamples. Open symbols are analyses for which ^{231}Pa and ^{230}Th ages were determined on different pieces of the same subsample; solid symbols are analyses for which both ages were determined on the same subsample. The dimensions of the symbols represent the errors in the analyses. The ^{230}Th analyses for the Devils Hole subsamples are from (*7*). All other ^{230}Th analyses were performed at Minnesota [either reported in (*5*) and (*6*) or are new data]. The curves represent "concordia," the locus of points for which ^{231}Pa and ^{230}Th ages are identical. Each diagram depicts a concordia curve appropriate for a marine initial $\delta^{234}U$ (150 per mil); (B) also depicts a concordia curve for an initial $\delta^{234}U$ value appropriate for Devils Hole (1800 per mil). The concordia curves are contoured (horizontal line segments) in age. Points that plot above and to the left of concordia have isotopic characteristics consistent with U loss, whereas those that plot below and to the right of concordia have characteristics consistent with U gain. Most of the Huon Peninsula points plot on or very close to concordia, indicating that the ages of most of these samples are accurate and supporting the conclusions of (*5*). The discordant Barbados samples all plot above concordia, consistent with diagenetic loss of U or gain of both Th and Pa. The ages of the concordant samples support a sea level chronology consistent with orbital forcing of the glacial-interglacial cycles (*6*). The Devils Hole samples are both concordant, supporting the accuracy of the Devils Hole chronology (*7*).

value greater than that of seawater must have been added. Plausible sources are high $\delta^{234}U$ ground waters, which have yet to be identified on Barbados (*15*) but are common elsewhere. Initial $\delta^{234}U$ values in altered Barbados corals tend to increase with age (*1*, *6*, *15*), so the high $\delta^{234}U$ component must have been added over time. The result of net U loss or Pa and Th gain and addition of a high $\delta^{234}U$ component is a shift in both ^{231}Pa and ^{230}Th ages to older values. If the same diagenetic processes affected the other Barbados samples with discordant ages, then ^{231}Pa and ^{230}Th ages of all Barbados samples with discordant ages are upper bounds on their true age.

If Pa and Th have been added, a plausible mechanism is transport from overlying materials either dissolved in ground water or adsorbed on small particles. If U has been lost, a plausible mechanism is multiple episodes of partial dissolution of coralline aragonite by ground water. Both Th and Pa are particle reactive and would tend to sorb onto the solid and remain, whereas the U would be transported away in solution. The high $\delta^{234}U$ component could be added from ground water by (i) precipitation of aragonite or (ii) addition of U to some minor component, such as organic material. Diagenetic aragonite is known to precipitate in crystallographic continuity with primary coralline aragonite (*16*). This hypothesis requires that ground water was sometimes undersaturated and sometimes saturated with respect to aragonite. The degree of aragonite saturation depends on the partial pressure of carbon dioxide imparted by overlying soil gases and the extent to which percolating ground waters have interacted with overlying carbonate, so varying degrees of aragonite saturation are possible. Because the organic content of corals is small [about 0.1% (*17*)], the organic U addition hypothesis would require high concentrations of U on organic matter (hundreds of parts per million) or high values of $\delta^{234}U$ of U assocated with organic matter (thousands of per mil) to account for the observed elevation in $\delta^{234}U$. Organic material could have high U concentrations (*17*), and high $\delta^{234}U$ values are not uncommon in ground waters; hence, either hypothesis is plausible.

The samples from Barbados with concordant ages indicate that sea level was relatively high 82.8 ± 1.0, 104.2 ± 1.2, 121.0 ± 2.1, 126.8 ± 2.5, and 193 ± 9 thousand years ago (*18*). The sea level highs marked by these corals correspond to oxygen isotope stages 5a, 5c, 5e (represented by both the 121.0 and the 126.8 ages), and 7.1, respectively. In all cases where samples with concordant and discordant ages were collected from the same terrace, maximum ages from the samples with discordant ages are consistent with the ages of the concordant samples. The ages are generally consistent with the times of high sea level inferred from the orbitally tuned oxygen isotope time scale of SPECMAP (*19*). The combined Pa-Th data support the conclusions of Gallup *et al.* (*6*), which were based solely on ^{230}Th ages (Fig. 4). A comparison (Fig. 4) of our sea level constraints with high-latitude Northern Hemisphere summer insolation values (*20*) shows that all of the high sea levels coincide with or slightly postdate times of high Northern Hemisphere insolation, consistent with the idea that changes in orbital geometry cause the Quaternary glacial-interglacial cycles.

In contrast, in Devils Hole calcite, the timing of the oxygen isotope shift from glacial to interglacial values around 140,000 years ago (Termination II) generally precedes the shift in insolation from glacial to interglacial values (Fig. 4) (*7*), suggesting that Termination II did not result from insolation rise (*7*). The timing of the Devils Hole record, which has come under intense scrutiny, was established by ^{230}Th dating. By correlating features from Devils Hole with those of several deep-sea oxygen iso-

Table 1. Various ages and initial $\delta^{234}U$ (calculated from measured $\delta^{234}U$ using ^{230}Th age) of corals and Devils Hole calcite. The $^{231}Pa/^{230}Th$ age equation is derived by combining the ^{231}Pa and ^{230}Th age equations and the known natural $^{238}U/^{235}U$ ratio to eliminate ^{235}U and ^{238}U from the denominators of the $^{231}Pa/^{235}U$ and $^{230}Th/^{238}U$ terms. A $^{231}Pa/^{230}Th$ age is analogous to a $^{207}Pb/^{206}Pb$ age in the U-Pb system. In addition to quoted errors, ^{231}Pa ages have systematic errors of ±0.6% in age as a result of uncertainty in the ^{231}Pa decay constant (*8*); this error is significantly smaller than that from the analytical error in each measurement. Likewise, the systematic error in ^{230}Th ages resulting from errors in decay constants is smaller than that from the analytical error in each measurement, except for samples older than about 200,000 years (*1*). Numbers in parentheses indicate the analytical error in the last digits. All measurements not indicated as being from (*6*) or (*7*) or from Los Alamos were performed at Minnesota. Roman numerals in the sample numbers denote replicate analyses on different fragments of the same hand specimen. For the Devils Hole samples, the quoted errors in the ages include the error in sampling position (*7*), which is significantly larger than analytical errors for DH-11-16mm ^{230}Th and ^{231}Pa ages (±1.4 ka for the ^{23}Pa age). Samples for which the ^{231}Pa age has "no solution" have $^{231}Pa/^{235}U > 1$. Sample VA-1 has $^{230}Th/^{238}U$ and $^{230}Th/^{231}Pa$ ratios higher than are possible by means of closed-system evolution.

Sample number	^{230}Th age (ka)	^{231}Pa age (ka)	$^{231}Pa/^{230}Th$ age (ka)	$\delta^{234}U_i$ (initial)
		Corals younger than 1000 years (representative analyses)		
FSL-2*	0.137(3)	0.138(7)†	−5(8)†	148.6(1.6)
BA-7*	0.973(5)	0.968(7)†	1.2(1.5)†	148.1(1.2)
		Papua New Guinea (representative analyses)		
HOB-EE-3*	9.910(40)	9.760(70)†	12.2(1.3)†	150.3(1.1)
51.5 m	13.040(50)	13.080(130)	12.5(1.6)	150.6(1.1)
		Barbados: Worthing Terrace		
FS-3*	82.9(0.4)	83.8(1.2)†	81.8(1.7)†	151.9(1.4)
FS-3	–	81.8(1.4)	84.2(2.0)‡	–
FS-8(I)	86.1(0.4)	89.5(1.3)	82.5(1.5)	165.5(1.4)
FS-8(II)	85.4(0.4)	86.2(1.0)	84.5(1.4)	163.2(1.4)
		Barbados: Ventnor Terrace		
FT-1(I)	103.1(0.5)	103.0(2.4)	103.4(2.2)	185.9(1.6)
FT-1(II)	105.4(0.6)	105.6(2.2)	105.9(2.0)	191.1(1.6)
		Barbados: Rendezvous Hill Terrace		
AFM-20	126.9(1.1)	126.8(2.5)	126.9(2.2)	165.7(1.7)
UWI-16*	132.0(0.9)	143(6)†	127.0(2.5)†	174.5(1.9)
FU-1(I)	122.3(0.7)	120.0(3.4)	123.7(2.5)	157.8(1.6)
FU-1(II)	122.6(0.7)	119.0(2.6)	125.0(2.1)	160.2(1.8)
FU-3	147.3(0.9)	No solution	119.4(2.3)	240.6(1.6)
		Barbados: "stage 7" terraces		
WAN-B2(I)*	191.7(1.6)	$190(^{+17}_{-12})$†	192.0(3.9)†	147.1(2.0)
WAN-B2(II)	193.1(1.6)	$197(^{+15}_{-11})$	192.3(3.3)	145.9(2.0)
WAN-B2(III)	190.2(1.5)	$195(^{+14}_{-11})$	189.1(3.1)	148.3(1.8)
WAN-B-7*	200.8(1.0) (*6*)	$185(^{+15}_{-11})$†	204.9(4.0)† (*6*)	152.3(2.0) (*6*)
WAN-B-8	203.6(1.8)	$262(^{+\infty}_{-33})$	197.2(3.2)	185.2(2.3)
WAN-B-5	217.9(2.1)	No solution	204.9(4.0)	218.5(2.4)
FY-2	206.1(1.8)	No solution	188.6(3.0)	215.6(2.3)
		Barbados: pre-"stage 7" terraces		
VA-1	No solution	>314	No solution	–
		Devils Hole: DH-11 subsamples		
16 mm*	80.6(2.5) (*7*)	82.5(2.8)†	79(5)† (*7*)	1790(13) (*7*)
188 mm*	354(6) (*7*)	$280(^{+\infty}_{-60})$†	358(13)† (*7*)	1808(33) (*7*)

*Subsample analyzed for $\delta^{234}U$ and $^{230}Th/^{238}U$ was different from that analyzed for $^{231}Pa/^{235}U$. †$^{231}Pa/^{235}U$ ratio measured at Los Alamos. ‡Calculated from $^{230}Th/^{238}U$ and $\delta^{234}U$ on the line above.

tope records, Imbrie *et al.* (*21*) established Devils Hole–based chronologies for several deep-sea sediment cores. Although the cores are from different sedimentary environments, the chronologies give similar sedimentation-rate anomalies before and during the penultimate deglaciation. Thus, either the Devils Hole chronology is inaccurate or analogous features in the Devils Hole and marine oxygen records may not correlate in time.

We tested the Devils Hole chronology (*22*) by dating splits of two subsamples of Devils Hole calcite (DH-11-16mm and DH-11-188mm) by the ^{231}Pa method (Table 1 and Figs. 3B and 4). The ^{231}Pa age of DH-11-16mm [82.5 ± 2.8 thousand years (ka)] was indistinguishable from its reported ^{230}Th age [80.6 ± 2.5 ka (*6*)], suggesting that the ages are accurate and that the subsample behaved as a closed system. The ^{230}Th age of DH-11-188mm is 354.1 ± 6.2 ka (*7*). This age is beyond the range of ^{231}Pa dating. Therefore, the ^{231}Pa/^{235}U activity ratio of this subsample should be one, unless it was open to chemical exchange. Our measured ^{231}Pa/^{235}U ratio is 0.9976 ± 0.0056, suggesting that the subsample behaved as a closed system over at least the last 250,000 years. If this small number of subsamples is representative of the rest of the vein, then the Devils Hole chronology is accurate. This result suggests that analogous features of the Devils Hole and marine oxygen isotope records may not have formed at the same time. Because the Devils Hole oxygen isotope signal may reflect regional temperatures, whereas the marine oxygen isotope record largely reflects the volume of continental ice sheets, different times of origin appear entirely possible. Temperatures near Devils Hole could have reached interglacial values before the Northern Hemisphere ice sheets melted to interglacial extents. This postulated relation is similar to the one established for the Bahamas, where regional climate became drier well before the Northern Hemisphere ice sheets melted during each of the last two deglaciations (*3*).

If the Devils Hole chronology is accurate, then the Termination II shift in oxygen isotope values apparently takes place before the insolation rise (Fig. 4) (*7*). One interpretation of this relation is that orbital forcing did cause Devils Hole Termination II. If so, (i) 65°N summer insolation is the wrong curve with which to compare Devils Hole temperature, (ii) the insolation calculation is off by a small but significant amount, or (iii) the temperature at Devils Hole increased nonlinearly in response to the increase in insolation during Termination II. With regard to the first possibility, one can choose insolation curves that match Devils Hole Termination II. For example, the Termination II rise in summer insolation for 80°N (*20*) matches closely the oxygen isotope shift at Devils Hole during Termination II. It is reasonable that high-latitude insolation should have some effect on mid-latitude climate. An energy-balance model of this relation during Termination II (*23*) lends some support to this hypothesis. Regarding the second possibility, a shift in calculated insolation of as little as 2000 years (to older values) would make most of the Termination II oxygen isotope and insolation rises coincident. Regarding the third possibility, modeling shows that one would not expect the climate's response to insolation changes to be either direct or proportional (*24*). If so, the initial part of the Termination II insolation rise could have resulted in a large regional rise in temperature near Devils Hole. In this case, most of the oxygen isotope shift could be attributed to a change in insolation. Alternately, it is still possible that there is no causal relationship between orbital forcing and Devils Hole Termination II (*7*). However, in view of the clear relation between sea level and insolation (Fig. 4), we consider that one or some combination of the other possibilities is more likely.

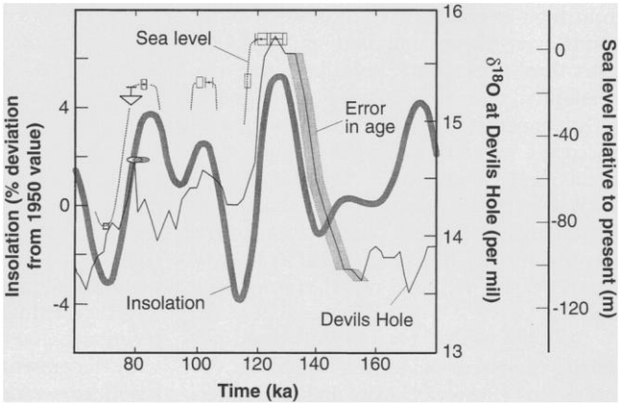

Fig. 4. Plot of summer solar insolation (*20*), Devils Hole $\delta^{18}O$ (*7*), and sea level [open boxes and dotted line (*6*)] versus time. For illustrative purposes, the width of the insolation curve corresponds to an error of ±1 ka. The stippled area on either side of the Devils Hole curve corresponds to quoted errors in ^{230}Th age (*7*) for that part of the curve. The ellipses indicate the $\delta^{18}O$ (*7*) of Devils Hole sample DH-11-16mm, its ^{231}Pa age (stippled ellipse) and ^{230}Th age (*7*) (open ellipse), and errors. The open boxes and arrow are sea level data and errors from (*6*), and the dashed line is inferred sea level. The solid dots with error bars are concordant sea level data from this study.

REFERENCES AND NOTES

1. J. H. Chen, R. L. Edwards, G. J. Wasserburg, *Earth Planet. Sci. Lett.* **80**, 241 (1986); R. L. Edwards, J. H. Chen, G. J. Wasserburg, *ibid.* **81**, 175 (1987).
2. R. L. Edwards, J. H. Chen, T.-L. Ku, G. J. Wasserburg, *Science* **236**, 1547 (1987); W.-X. Li *et al.*, *Nature* **339**, 534 (1989); E. Bard, B. Hamelin, R. G. Fairbanks, *ibid.* **346**, 456 (1990); J. H. Chen, H. A. Curran, B. White, G. J. Wasserburg, *Geol. Soc. Am. Bull.* **103**, 82 (1991); B. Hamelin, E. Bard, A. Zindler, R. G. Fairbanks, *Earth Planet. Sci. Lett.* **106**, 169 (1991); E. Bard, R. G. Fairbanks, B. Hamelin, A. Zindler, C. T. Hoang, *Geochim. Cosmochim. Acta* **55**, 2385 (1991); M. Stein *et al.*, *ibid.* **57**, 2541 (1993); G. M. Henderson, A. S. Cohen, R. K. O'Nions, *Earth Planet. Sci. Lett.* **115**, 65 (1993); C. H. Stirling, T. M. Esat, M. T. McCulloch, K. Lambeck, *ibid.* **135**, 115 (1995); N. C. Slowey, G. M. Henderson, W. B. Curry, *Nature* **383**, 242 (1996).
3. D. A. Richards, P. L. Smart, R. L. Edwards, *Eos* **73**, 172 (1992); *Nature* **367**, 357 (1994).
4. E. Bard, B. Hamelin, R. G. Fairbanks, A. Zindler, *Nature* **345**, 405 (1990); E. Bard *et al.*, *Nucl. Instrum. Methods B* **52**, 461 (1990); E. Bard, M. Arnold, R. G. Fairbanks, B. Hamelin, *Radiocarbon* **35**, 191 (1993).
5. R. L. Edwards *et al.*, *Science* **260**, 962 (1993).
6. C. D. Gallup, R. L. Edwards, R. G. Johnson, *ibid.* **263**, 796 (1994).
7. I. J. Winograd *et al.*, *ibid.* **258**, 255 (1992); K. R. Ludwig, *ibid.*, p. 284.
8. J. Robert, C. F. Miranda, R. Muxart, *Radiochim. Acta* **11**, 104 (1969); M. R. Schmorak, *Nucl. Data Sheets* **21**, 91 (1977).
9. G. W. Wetherill, *Trans. Am. Geophys. Union* **37**, 320 (1956); G. R. Tilton, *J. Geophys. Res.* **65**, 2933 (1960); G. J. Wasserburg, *ibid.* **68**, 4823 (1963).
10. C. Allegre, *C. R. Acad. Sci. Paris* **259**, 4086 (1964) discusses Pa-Th concordia diagrams and models Pa-Th systematics for single-stage U gain. The behavior of Pa-Th during other types of open-system behavior is discussed by H. Cheng, R. L. Edwards, M. T. Murrell, and T. M. Benjamin, unpublished data.
11. W. M. Sackett, thesis, Washington Univ., St. Louis (1958); T.-L. Ku, *J. Geophys. Res.* **73**, 2271 (1968).
12. D. A. Pickett, M. T. Murrell, R. W. Williams, *Anal. Chem.* **66**, 1044 (1994).
13. Methods for U and Th analysis at Minnesota are described in (*5, 6*). Pa methods at Los Alamos and Minnesota are essentially those described in (*12*). Samples of 1.4 to 4.0 g were dissolved and aliquoted into a fraction for Pa analysis and one for U or U and Th analysis. The Pa aliquot was spiked with a ^{233}Pa tracer milked from a solution of ^{237}Np. The Los Alamos tracer was calibrated with a solution of Table Mountain Latite [S. J. Goldstein, M. T. Murrell, D. R. Janecky, *Earth Planet. Sci. Lett.* **96**, 134 (1989)], which is known to be in secular equilibrium for ^{230}Th, ^{234}U, and ^{226}Ra. It was also calibrated by γ-counting. The two techniques agreed to better than 1%. The Minnesota tracer was calibrated with a solution of a zircon that records concordant U-Pb ages [the zircon from the Piper Gulch Granodiorite: Y. Asmeron, R. E. Zartman, P. E. Damon, M. Shafigullah, *Geol. Soc. Am. Bull.* **102**, 961 (1990)] and is known to be in secular equilibrium for ^{234}U and ^{230}Th on the basis of gravimetric U and Th standards and accepted decay constants. A Pa-rich fraction was isolated by iron hydroxide precipitation and ion exchange. The sample was loaded on a single zone-refined Re filament with colloidal graphite. At temperatures of 1850° to 1950°C, ^{231}Pa/^{233}Pa ratios were measured on an electron multiplier in pulse-counting mode. Ionization efficiencies approached 1%. One can routinely mea-

sure 1.3 billion atoms of ^{231}Pa (500 fg, the amount in 0.5 g of coral in secular equilibrium) to ±0.5% (2σ). As a test of the accuracy of the tracer calibrations and the mass spectrometric measurements, each laboratory's tracer was used to calibrate a ^{231}Pa standard solution. The calibrations agreed.
14. R. L. Edwards, F. W. Taylor, G. J. Wasserburg, *Earth Planet. Sci. Lett.* **90**, 371 (1988).
15. J. L. Banner, G. J. Wasserburg, J. H. Chen, J. D. Humphrey, *ibid.* **107**, 129 (1991).
16. J. M. A. Chappell and H. A. Polach, *Quat. Res.* **2**, 244 (1972).
17. S. A. Wainwright, *Q. J. Micr. Sci.* **104**, 169 (1963); A. J. Ameil, D. S. Miller, G. M. Friedman, *Sedimentology* **20**, 523 (1973).
18. Each quoted age is the average of all ^{230}Th and ^{231}Pa ages for each sample with concordant ages. Each error is the error in ^{231}Pa age, which is, for each sample, larger than the error in ^{230}Th age. For samples with more than one ^{231}Pa age determination, the error was calculated by combining the errors quadratically and dividing by the number of ^{231}Pa age determinations. It is possible to have a concordant age even if the sample has behaved as an open system, if open-system behavior caused the isotopic composition to shift along concordia. An example of this type of behavior would be U loss for a material younger than 10,000 years. In this case, as the U is lost, the isotopic composition of the material will shift along a line with a slope very close that of concordia. In the case of the Barbados corals, all of the materials are significantly older than 10,000 years and would not be affected by this sort of artifact.
19. J. Imbrie *et al.*, in *Milankovitch and Climate*, A. Berger, J. Imbrie, G. Kukla, B. Saltzman, Eds. (Reidel, New York, 1984), part 1, pp. 269–306.
20. A. L. Berger, *Quat. Res.* **9**, 139 (1978); and tabulated values supplied by A. L. Berger.
21. J. Imbrie, A. C. Mix, D. Martinson, *Nature* **363**, 531 (1993).
22. Other questions regarding the accuracy of the Devils Hole chronology include the possibility that there was some initial ^{230}Th in the calcite resulting in artificially high ages [N. J. Shackleton, *Nature* **362**, 596 (1993); R. L. Edwards and C. D. Gallup, *Science* **259**, 1626 (1993)]. Recent data argue against this possibility [K. R. Ludwig, K. R. Simmons, I. J. Winograd, B. J. Szabo, A. C. Riggs, *Science* **259**, 1626 (1993)]. Another concern (*6*) was that if the growth rate of Devils Hole calcite varied, linear interpolation of ages between dated subsamples would lead to inaccuracy. Recent data again argue against this artifact (K. R. Ludwig, personal communication).
23. T. J. Crowley and K.-Y. Kim, *Science* **265**, 1566 (1994).
24. See, for example, W. R. Peltier and W. T. Hyde, *J. Atmos. Sci.* **44**, 1351 (1986).
25. We thank D. A. Pickett, who helped initiate this project; J. A. Hoff, for discussions and technical help; C. D. Gallup and R. G. Johnson, who helped with the Barbados field program; A. L. Bloom and J. M. A. Chappell, who led the 1988 field expedition to Papua New Guinea; C. Allegre, who brought the early Pa-Th concordia work to our attention; and K. R. Ludwig, I. J. Winograd, F. W. Taylor, Y. Asmerom, and R. K. Mathews, who contributed samples. This work was supported by the Donors of The Petroleum Research Fund, administered by the American Chemical Society; NSF grants OCE-9402693, OCE-9500647, EAR-9512334, and EAR-9406183 to R.L.E.; and a U.S. Department of Energy, Office of Basic Energy Sciences, Geosciences Research Program grant to M.T.M. and S.J.G.

30 December 1996; accepted 25 March 1997

Effect of Low Glacial Atmospheric CO_2 on Tropical African Montane Vegetation

Dominique Jolly* and Alex Haxeltine

Estimates of glacial-interglacial climate change in tropical Africa have varied widely. Results from a process-based vegetation model show how montane vegetation in East Africa shifts with changes in both carbon dioxide concentration and climate. For the last glacial maximum, the change in atmospheric carbon dioxide concentration alone could explain the observed replacement of tropical montane forest by a scrub biome. This result implies that estimates of the last glacial maximum tropical cooling based on treeline shifts must be revised.

Atmospheric general circulation model simulations for the last glacial maximum (LGM; 18,000 ^{14}C years before the present) have been used to study the effects of low greenhouse gas concentration, extended ice-sheet distribution, and lowered sea-surface temperatures on climate and vegetation (*1*, *2*). Knowledge of tropical paleoclimates is crucial for evaluating the reliability of LGM climate model simulations, and such evaluations can check the models' ability to simulate future climates (*3*, *4*). Pollen data from East Africa have been used to estimate the climate of the tropics at the LGM (*5*–*7*). For the LGM, East African pollen records show that cool grassland and xerophytic scrub increased at the expense of tropical montane forests (*2*). However, the occurrence of trees such as *Podocarpus* and *Olea* in low abundances suggests that forest refuges persisted near some sites (*5*, *8*). Tree lines also dropped in elevation by about 1000 m. On the basis of analogs with modern pollen assemblages, these changes have been attributed to a combination of cooler (4°C lower) and drier (30% less precipitation) conditions at the LGM than at present (*9*, *10*). This magnitude of cooling was in better agreement with climate model simulations (*11*) than with empirical estimates derived from continental-scale paleoenvironmental data (*12*). Recent δ^{13}C measurements on glacial-age sediments from high-elevation sites indicate that C_4 plants were more abundant at the LGM than they are today. These data raise the possibility that the lowered atmospheric CO_2 concentration (*13*) may have influenced the vegetation through physiological effects (*14*). We used the vegetation model BIOME3 (*15*) to examine what changes in CO_2, temperature, and precipitation might account for the observed characteristics of East African montane vegetation at the LGM.

BIOME3 (*15*, *16*) is a process-based terrestrial biosphere model that simulates the interacting effects of climate and atmospheric CO_2 levels on vegetation distribution and biogeochemistry (*15*, *17*). The model includes a photosynthesis scheme that simulates acclimation of plants to changed atmospheric CO_2 levels by optimization of nitrogen allocation to foliage and by accounting for the effects of CO_2 on net assimilation, stomatal conductance, leaf area index, and ecosystem water balance (*18*).

The Kashiru site (in Burundi) provides a well-dated, high-resolution LGM pollen record (*8*). Today, the Kashiru peat bog is located in the potential afromontane forest zone and contains *Macaranga*, *Podocarpus*, *Olea*, *Syzygium*, Araliaceae, and *Entandrophragma* (*19*). During the LGM, the site was occupied by a xerophytic association (the ericaceous belt) dominated by Gramineae, Ericaceae, *Artemisia*, and temperate families such as Caryophyllaceae, Dipsacaceae, Cruciferae, and Ranunculaceae (*8*).

We obtained current climate data for the 0.5° grid cell containing Kashiru (13°28′S, 29°34′E, 2240-m elevation) from an updated version of a global climate database (*20*). The monthly mean climate values were adjusted to be consistent with available data (*9*) on annual mean temperature and precipitation at Kashiru (15.8°C and 1460 mm/year). We assumed that the soils have a medium texture. Atmospheric pressure was estimated as 7.7×10^4 Pa (*21*) and was used to calculate the partial pressures of O_2 and CO_2. Absolute minimum temperature was estimated from a global regression of absolute minimum temperature on mean temperature of the coldest month (*22*).

A simulation with the preindustrial atmospheric CO_2 level (*23*) and present climate (Fig. 1A) resulted in tropical montane forest (dominated by broad-leaved evergreen trees) at the Kashiru site, consistent with the present natural vegetation. A transition to evergreen microphyllous (ericaceous) scrub, similar to the LGM vegetation, was predicted when annual temperature was reduced by a minimum of 6.5°C. A

Global Systems Group, Department of Ecology, Lund University, Ecology Building, S-223 62 Lund, Sweden.

*To whom correspondence should be addressed. E-mail: djolly@planteco.lu.se